JOURNAL OF SOLID STATE CHEMISTRY **125,** 47–53 (1996)
ARTICLE NO. 0263

Synthesis, Structural Characterization, and Electronic Properties of the $LaNi_{1-x}W_xO_3$ ($O \leq x \leq 0.25$) Perovskite-like System

I. Alvarez,* J. L. Martínez,† M. L. Veiga,* and C. Pico*,[1]

*Depto. Química Inorgánica I, Facultad de Ciencias Químicas, Universidad Complutense, 28040 - Madrid, Spain; and †Instituto de Ciencias de los Materiales, Sede B, CSIC, Campus de la Universidad Autónoma, 28049 - Madrid, Spain

Received November 29, 1995; in revised form April 29, 1996; accepted May 2, 1996

The structural characterization and electronic properties for the $LaNi_{1-x}W_xO_3$ perovskite-like system are reported. Neutron and X-ray powder diffraction data suggest that for the $x > 0$ phases, an orthorhombic symmetry (space group *Pbnm*) is adopted showing that Ni and W atoms are placed at random. The evolution of the cell-parameters is in agreement with the different size of the concerned cations in each case. The electronic measurements between 5 and 950 K show a temperature dependence of conductivity very sensitive to the composition. For the $0 \leq x \leq 0.20$ compounds, a conductivity variation very close to metallic behavior is observed whereas the mixed oxide with $x = 0.25$ behaves as a semiconductor. Both conductivity data and Seebeck coefficient measurements are interpreted on the basis of a correlated system in which a metal to insulator transition takes place as a function of temperature and composition. An schematic band model consistent with both the electronic properties and structural features is proposed.

INTRODUCTION

The electronic and magnetic properties of mixed-valent oxides with perovskite and related structures, which exhibit metal–insulator (M–I) transitions as a function of composition or temperature have been extensively studied in recent past years (1–10). The great current interest displayed by these type of materials is due in part to the occurrence of high T_c superconductivity in some examples of copper oxide systems in this mixed-valence regime (11). In various cases, the M–I transition was reported to be composition driven (10), whereas in some systems, as $RNiO_3$ (R = rare earth), it was reported to be temperature and structure driven (7). In general, the electrical behavior of perovskite (or related)-type materials is explained in terms of localized to collective electron transitions and is often interpreted on the basis of conduction models implying hopping activation of carriers when the M–I transition is crossover (9, 10).

The compound $LaNiO_3$, in which all the Ni cations are in the trivalent state, is a rhombohedrically distorted perovskite phase, known to be a narrow band metallic conductor (12). It has been shown that compounds with the general formula $La_{n+1}Ni_nO_{3n+1}$ (3), in which Ni is in the mixed-valent state, can be stabilized. This system shows M–I transitions as a function of temperature and composition. The progressive multilayer structure (from La_2NiO_4 to $LaNiO_3$ Ruddelson–Popper series) together with the Ni^{2+}/Ni^{3+} relative ratio (i.e., the possibility of hole creation, the change in itinerant electrons fraction, etc.) were the most representative features taken into account in order to interpret both magnetic and electrical properties.

We have been interested in stabilizing the Ni mixed-valent state but conserving the perovskite-type structure. In this sense, we have carried out the synthesis, structural characterization, and some studies concerning the transport properties of $LaNi_{1-x}W_xO_3$ ($0 \leq x \leq 0.25$). Formally, for $x = 0$ only Ni^{3+} is present and for $x = 0.25$ this element is stabilized as Ni^{2+}. From neutron and X-ray powder diffraction data a correct structural characterization has been done, and a clear relationship Ni oxidation state and transport properties can be addressed.

EXPERIMENTAL

It has been previously stated (13) that the stabilization of Ni^{3+} cations is difficult to achieve at high temperatures, because the reduction of Ni^{2+} takes place. As the ceramic method usually requires high temperatures, it is usual to carry out the synthesis of Ni^{3+}-containing compounds via low-temperature methods. Although we have reported previously that for $x \geq 0.20$ it is possible to obtain the materials by using the ceramic method (14), all the mixed oxides concerning the study that we report here were prepared by the sol–gel method in order to assure the comparison of the obtained data.

The synthesis of $LaNi_{1-x}W_xO_3$ ($0 \leq x \leq 0.25$) was carried out starting from aqueous solutions of the metal nitrates

0022-4596/96 $18.00

$La(NO_3)_3 \cdot 6H_2O$ and $Ni(NO_3)_2) \cdot 6H_2O$ and WO_3 in a stoichiometric ratio. About 4 g of the metal nitrates and oxide were added to a mixture of 10 g of citric acid and 4 ml of ethyleneglycol. These ingredients were mixed together and drops of HNO_3 were added to catalyze the gel formation. The excess nitric acid was boiled off and the gel was slowly decomposed by heating up to 400°C. The remaining black powders were intimately mixed and heated in several steps up to temperatures ranging from 800 to 1000°C in air. During the thermal treatment, the samples were reground in each step and the process was monitored by X-ray diffraction until single phases were obtained.

The X-ray diffraction patterns were recorded using a Siemens Kristallofex 800 diffractometer and a D-500 goniometer with nickel-filtered copper radiation. Both a step scan of 0.04 and a counting time of 15 s for each step were employed. The goniometer was controlled by a DACO-MPV2 computer.

The neutron powder diffraction data were recorded at room temperature and 1.7 K on the D2B powder diffractometer (λ = 1.5945 Å) at the Institute Laue-Langevin in Grenoble. The neutron and X-ray diffraction data were analyzed by the Rietveld method using the Fullprof program (15). A pseudo-Voigt function was chosen to generate the line shape of the diffraction peaks.

For the electronic resistivity measurements pelletized samples were sintered at temperatures somewhat smaller than the respective synthesis temperatures. Pycnometric measurements evidenced that for all the samples the densities were higher than 90% of the crystallographic values. The electronic resistivity was measured by using the Van der Pauw method (16), which avoids the contact effects. Contacts were made by covering with platinum or silver paint the circular faces of the sample disks. Seebeck coefficient measurements were made in an apparatus set up and checked in our laboratory.

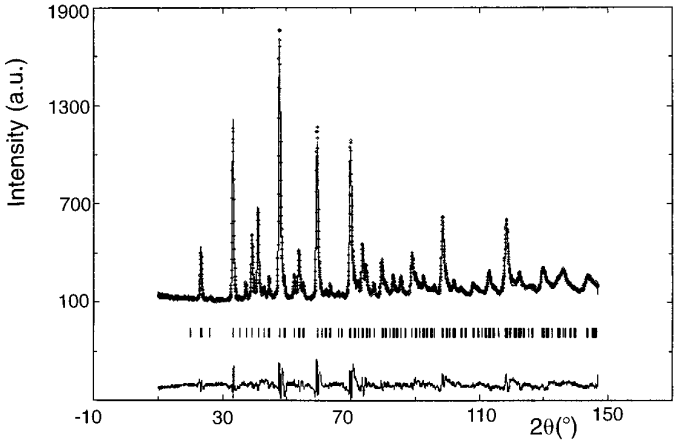

FIG. 1. Observed (upper dotted line), calculated (lower line), and difference (vertical lines) neutron diffraction profiles for $LaNi_{0.80}W_{0.20}O_3$.

RESULTS AND DISCUSSION

1. Structural Characterization

X-ray diffraction data for all the title compounds were analyzed by means of the Rietveld method. The $x = 0$ phase was found to have a rhombohedrically distorted perovskite structure, space group *R3c* (No. 167), with hexagonal parameters a = 5.446(1) Å and c = 13.154(2) Å. These lattice parameters are close to those reported earlier (6).

The diffraction data of the remaining mixed oxides $LaNi_{1-x}W_xO_3$ ($0.05 \leq x \leq 0.25$) are characteristic of the perovskite structure and can be indexed and refined considering an orthorhombic symmetry and space group *Pbnm* (No. 62).

Figure 1 shows, as an example, the observed and calculated neutron diffraction profiles for $LaNi_{0.80}W_{0.20}O_3$, at room temperature, and in Table 1 the crystal data and

TABLE 1
Crystal Data and Agreement Factors for $x = 0.20$ at 1.7 K (Boldface) and 300 K (Lightface)

Atom	Site	x	y	z	β	Occup.
La	4*c*	0.015(1)	0.0416(5)	0.25	1.8(2)	
		0.015(1)	**0.0419(5)**	**0.25**	**1.7(2)**	
Ni/W	4*b*	0.5	0	0	0.8(1)	
					0.6(1)	
O(1)	8*d*	0.291(1)	0.284(1)	0.0365(4)	1.8(3)	1.01(1)
		0.291(1)	**0.286(1)**	**0.0376(7)**	**1.7(3)**	**1.01(1)**
O(2)	4*c*	−0.069(1)	0.501(1)	0.25	1.3(4)	0.50(1)
		−0.070(1)	**0.500(1)**	**0.25**	**1.0(2)**	**0.50(1)**

Note. a = 5.5691(9) Å, b = 5.5757(9) Å, c = 7.856(1) Å; **a = 5.560(1) Å, b = 5.571(1) Å, c = 7.845(1) Å.** R_{wp} = 8.4, R_p = 6.4, R_B = 6.6, χ^2 = 6.5; **R_{wp} = 8.9, R_p = 6.8, R_B = 7.4, χ^2 = 7.2.**

TABLE 2
Most Representative Bond Lengths for $LaNi_{0.80}W_{0.20}O_3$ at 1.7 K (Boldface) and 300 K (Lightface)

La–O(1)	2.646(7) × 2	(Ni/W)–O(1)	1.986(6) × 2
	2.643(7) × 2		**1.997(6) × 2**
La–O(1)	2.455(7) × 2	(Ni/W)–O(1)	2.040(6) × 2
	2.439(7) × 2		**2.029(6) × 2**
La–O(1)	2.750(7) × 2	(Ni/W)–O(2)	2.002(2) × 2
	2.749(7) × 2		**2.000(1) × 2**
La–O(2)	2.606(8)	Mean	2.01
	2.599(8)		**2.01**
La–O(2)	2.49(1)	Shannon	2.04
	2.48(1)		**2.04**
Mean	2.60	$\theta_1(O_1–Ni/W–O_1)$	156.3°
	2.59		**155.6°**
Shannon	2.56	$\theta_2(O_2–Ni/W–O_2)$	157.8°
	2.56		**157.4°**

agreement factors for both this refinement and that correspondent for 1.7 K are gathered. As it can be observed from the oxygen occupancy factors, the stoichiometry of this compound could be effectively assumed. From the agreement between the observed and calculated profiles as well as the R factors obtained we can accept as valid the proposed model. The most representative bond lengths for $LaNi_{0.80}W_{0.20}O_3$ are given in Table 2. The mean values and the sums of the ionic radii, as given by Shannon (17), are included and they agree reasonably. The $\theta_1(O_1–Ni/W–O_1)$ and $\theta_2(O_2–Ni/W–O_2)$ angles are also presented and it can be observed that both angles increase at temperature increases. This fact will be decisive in the electronic properties of the title materials, as commented below.

The X-ray diffraction data for the other members of the title series were also refined by the Rietveld method, showing that they are all isostructural. As an example, Fig. 2 shows the observed and calculated X-ray diffraction

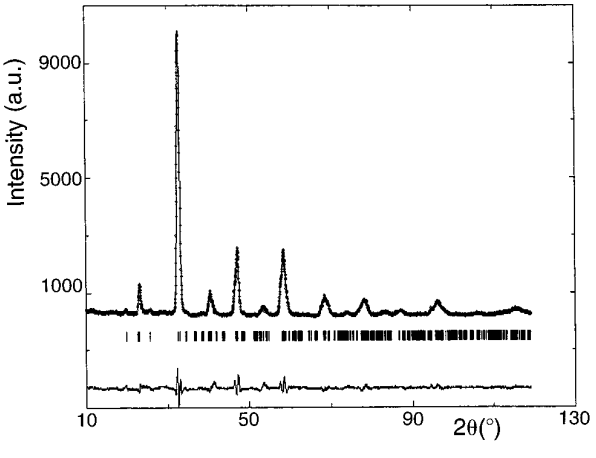

FIG. 2. Observed (upper dots line), calculated (lower line), and difference (vertical lines) X-ray diffraction profiles for $LaNi_{0.90}W_{0.10}O_3$.

TABLE 3
Crystal Data and Agreement Factors for $LaNi_{0.90}W_{0.10}O_3$

Atom	Site	x	y	z
La	4*c*	−0.003(2)	0.0230(7)	0.25
Ni/W	4*b*	0.5	0	0
O(1)	8*d*	0.218(4)	0.251(4)	−0.043(1)
O(2)	4*c*	0.064(8)	0.386(7)	0.25

Note. a = 5.423(2) Å, b = 5.499(2) Å, c = 7.793(3) Å; R_{wp} = 13.8, R_p = 9.9. R_B = 5.8, χ^2 = 9.2.

profiles for the $x = 0.10$ compound and in Table 3 the crystal data and agreement factors obtained in the refinement are gathered. Table 4 shows the cell parameters for all the members. From the atomic coordinates we have calculated the most representative bond distances for each case. In Fig. 3 the variation and mean distances (W/Ni)–O with the composition are shown. The observed behavior is in good agreement with the differences in ionic radii between the Ni^{3+} (0.56 Å in low-spin configuration) and the Ni^{2+} (0.69 Å) or W^{6+} (0.60 Å) cations, all in octahedral coordination (values taken from Shannon, Ref. 17). As x increases, the mean size of cations placed at B sites increases and so does the cell volume.

The above results allow us to describe the structure of these perovskites as built from $(Ni/W)O_6$ octahedra which share all their corners with analogous units; i.e., the cations located in B sites, Ni^{2+}, Ni^{3+}, and W^{6+}, are randomly distributed. In this picture, interactions of the type Ni^{2+}–O–Ni^{2+}, Ni^{2+}–O–Ni^{3+}, Ni^{3+}–O–Ni^{3+}, etc. are all possible. It is also necessary to have in mind the possibility of Ni–W interactions, via oxygen anions.

2. *Conductivity Measurements*

The electronic conductivity variation with temperature for the $LaNi_{1-x}W_xO_3$ perovskites has been measured in the temperature range 5–950 K, using two different apparatuses which are able to cover the interval between 5 and 300 K and between 300 and 950 K, respectively. Figure 4 (a and b) shows separately the variation of ln σ vs $1/T$ for the above temperature ranges (both scales have been

TABLE 4
Cell Parameters and Cell Volume for $LaNi_{1-x}W_xO_3$

x	a (Å)	b (Å)	c (Å)	V (Å^3)
0	5.446(1)	5.446(1)	13.154(1)	338.1
0.05	5.419(2)	5.494(2)	7.699(4)	229.2
0.10	5.423(2)	5.499(2)	7.793(3)	232.3
0.15	5.489(1)	5.564(1)	7.887(1)	240.8
0.20	5.5691(9)	5.5757(9)	7.856(1)	243.9
0.25	5.560(1)	5.594(1)	7.918(1)	246.3

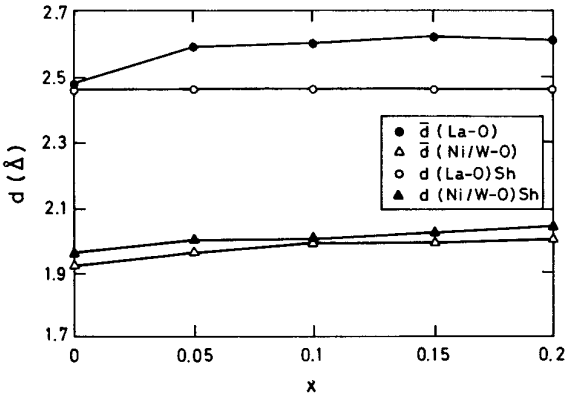

FIG. 3. Variation of mean bond distances with composition. The variation of Shannon distances is also shown.

chosen in order to visualize and compare the electronic behavior of the whole series). As can be observed, the temperature dependence of the conductivity is very sensitive to the composition. For $0 \leq x \leq 0.20$, a conductivity variation very close to metallic behavior is observed whereas the compound with $x = 0.25$ behaves as a semiconductor. Let us consider separately both composition domains.

(*a*) *Compounds with* $0 \leq x \leq 0.20$. $LaNiO_3$ (that is, $x = 0$) is known to behave as a metal down to 0.4 K (12). This behavior was interpreted in terms of a conduction band built from the hibridation of e_g nickel semioccupied orbitals (in low-spin configuration) and p oxygen orbitals (18). In this sense, this material has been classified as a low "W" semimetal (where "W" is the bandwidth), i.e., a highly correlated metal. The resistivity value obtained for this oxide at room temperature is $0.9 \times 10^{-3}\ \Omega \cdot$ cm, similar to those reported previously in the literature (9, 12). This is a high value for the resistivity of a metal and this fact, together with the enhancement of conductivity below ~150 K, has been interpreted in terms of an important electronic correlation as commented above.

For the $x = 0.05$ material, metallic behavior is observed down to ~50 K. Below this temperature a transition to the insulating state takes place, as it can be deduced when the variation of resistivity vs temperature is represented (Fig. 5). As a general trend, the conductivity values decrease as x increases and this seems to be a consequence of the progressive localization of the atomic levels or, alternatively, the progressive decreasing of the bandwidth. Finally, for $0.10 \leq x \leq 0.20$, the conductivity shows a monotonic variation in the whole temperature range studied. These phases ($x = 0.10$ and 0.20) show an almost linear temperature dependence of the conductivity below ~380 K and ~400 K, respectively. The conductivity data follow a power law equation of the type

$$\sigma(T) = \sigma_0(0) + \sigma_1 \cdot T^{\alpha}. \qquad [1]$$

The parameters which better fit Eq. [1] are gathered in Table 5. This kind of dependence is not very usual in mixed oxides and has been previously found in systems near a M–I transition (19). Figures 6 and 7 show the temperature dependence of the conductivity for the $x = 0.10$ and $x = 0.20$ phases, respectively, in the whole temperature range measured. In both cases we have concluded that the temperature variation of the conductivity is weaker above a certain temperature. For the $x = 0.20$ member, the conductivity is nearly temperature independent above ~400 K, whereas for the $x = 0.10$ compound a transition to the metallic state is effectively detected above ~380 K.

(*b*) *Compound with* $x = 0.25$. The compound of nominal composition $LaNi_{0.75}W_{0.25}O_3$ behaves as a semiconductor in the whole temperature range studied. The conductiv-

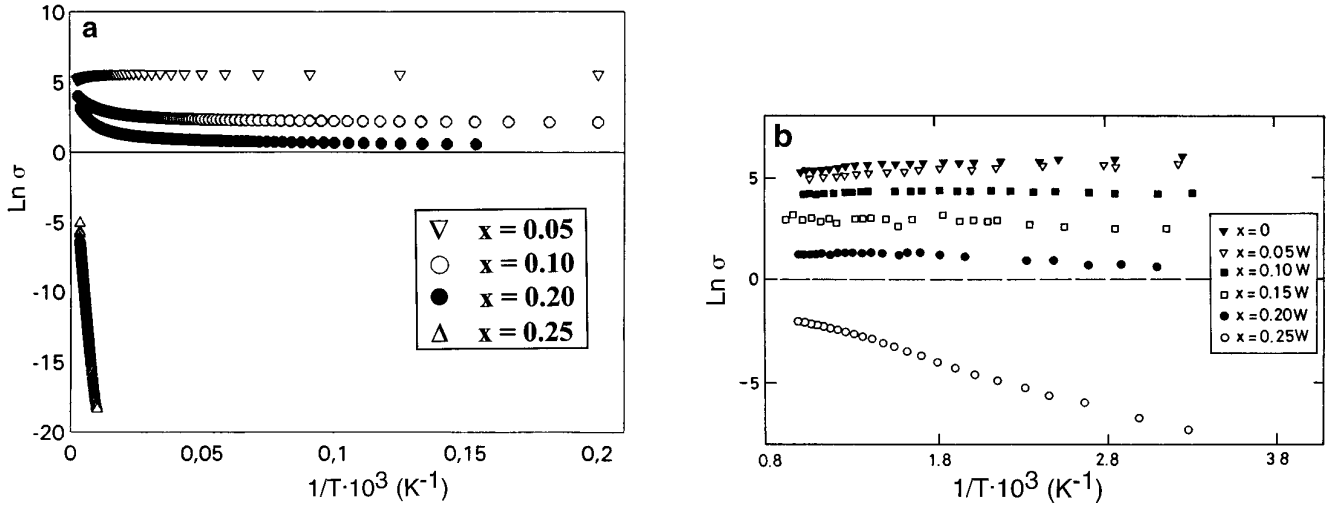

FIG. 4. Variation of ln σ vs $1/T$ (a) in the 5–300 K temperature range and (b) in the 300–950 K temperature range.

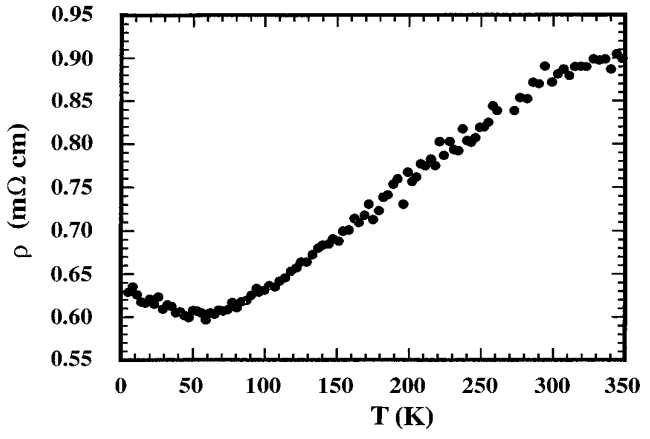

FIG. 5. Variation of resistivity vs temperature for $LaNi_{0.95}W_{0.05}O_3$.

ity data for this material were fitted to an exponential law as

$$\sigma = (A/T) \cdot \exp(-E/kT), \qquad [2]$$

which is usually applied to a small polaron hopping mechanism. In Eq. [2], E is the activation energy related to the hopping process, A is the preexponential factor, and k is the Boltzmann constant. Figure 8 shows the linear variation of $\ln(\sigma \cdot T)$ vs T^{-1} for the $x = 0.25$ phase, which agrees well with the above assumption, and the activation energy obtained for this material was 0.16 eV.

3. Seebeck Measurements

In order to evaluate both the predominant activation process (mobility or carriers concentration) and the sign of majority carriers, we have measured the variation of the Seebeck coefficient with temperature for $LaNi_{1-x}W_xO_3$ ($0.05 \le x \le 0.25$) in the temperature range 300–950 K.

Figure 9 shows the variation of the Seebeck coefficient with inverse temperature for all the series members. The compositors given by $x \le 0.15$ have negative values for this coefficient, thus suggesting that the conduction process is mainly due to electrons, whereas for the $x \ge 0.20$ materials, always positive values were found, which are indicative that holes are predominant as charge carriers. These results are in agreement with the Ni^{2+}/Ni^{3+} relative amounts present in the respective compounds.

On the other hand, the Seebeck coefficient at room temperature for the $LaNiO_3$ material has been reported to be $\sim -18\ \mu V/K$. In the $x \le 0.15$ composition range, the

TABLE 5
Fitting Parameters of the Conductivity for the $x = 0.10$ and $x = 0.20$ Compounds

Compound	σ_0 (S/cm)	σ_1 ($S \cdot cm^{-1} \cdot K^{-\alpha}$)	α
$LaNi_{0.90}W_{0.10}O_3$ (M)	6.4	0.19	0.97
$LaNi_{0.80}W_{0.20}O_3$ (A)	1.6	3.72×10^{-3}	1.58

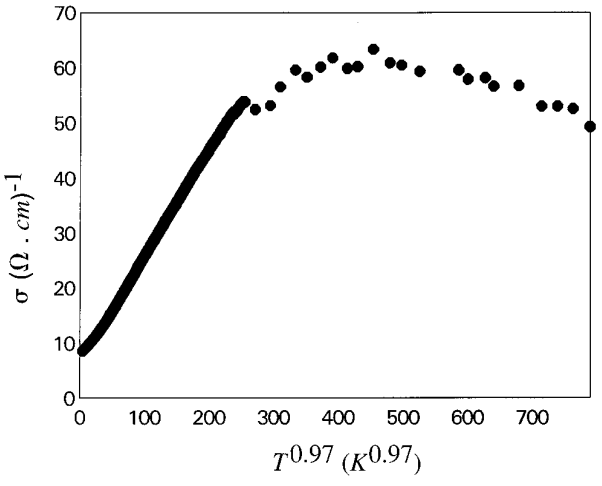

FIG. 6. Conductivity variation vs $T^{0.97}$ for $LaNi_{0.90}W_{0.10}O_3$.

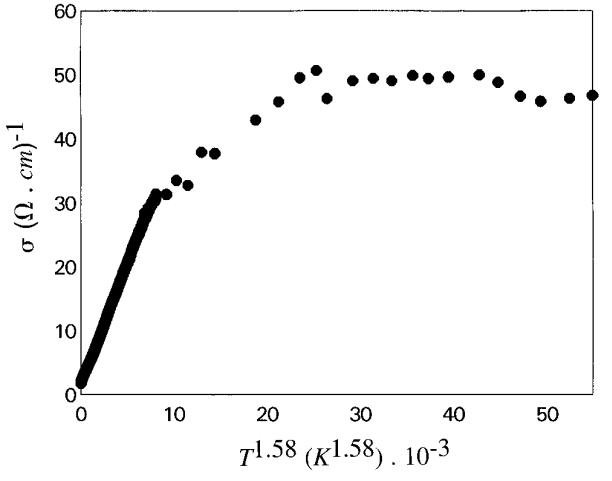

FIG. 7. Conductivity variation vs $T^{1.58}$ for $LaNi_{0.80}W_{0.20}O_3$.

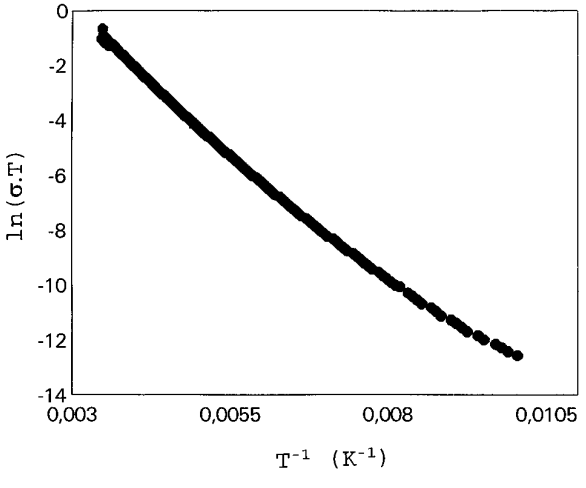

FIG. 8. Variation of $\ln(\sigma \cdot T)$ vs $1/T$ for $LaNi_{0.75}W_{0.25}O_3$.

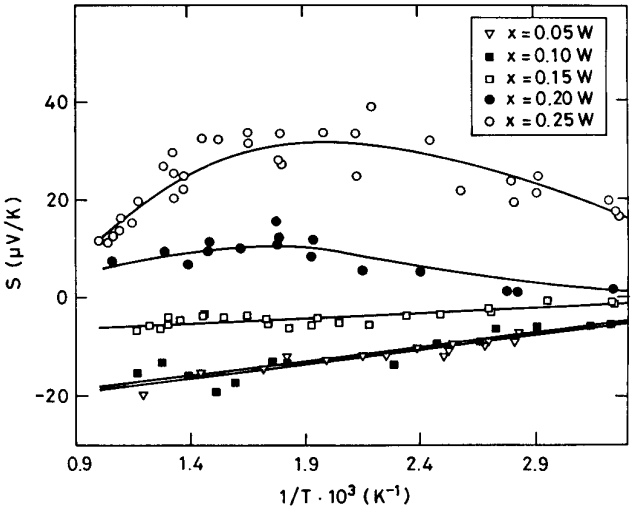

FIG. 9. Variation of the Seebeck coefficient with $1/T$ in the 300–950 K temperature range.

measured absolute values were always smaller than 20 μV/K. This order of magnitude has been pointed out as a typical one for metallic behavior (20).

For the $x \geq 0.20$ phases, the Seebeck values measured were much smaller than those usually found in nondegenerated semiconductors, $\sim 10^2$ μV/K, following the criterion of Goodenough for a hopping mechanism (21). This result, together with the nearly temperature independent behavior of the Seebeck coefficient, is in good agreement with a small polaron hopping of carriers, mainly driven by a mobility activation and with a charge carrier concentration almost constant.

Taking into account that the conductivity and Seebeck coefficient measurements suggested a hopping model for the conduction process in the $x = 0.25$ phase, we have applied the Heikes formula (22) to the data. Assuming only one polaron is allowed in a given site and that both the spin and orbital degeneracy can be neglected, Heikes derived the following expression for the Seebeck coefficient

$$S = \pm(k/e) \cdot \{\ln[(1 - x)/x] + S^*/K\}, \qquad [3]$$

where + and − indicate p or n behavior, respectively, k is the Boltzmann constant, x is the fraction of occupied sites, and S^* is the vibrational entropy. In general terms, it is assumed that S^* is small enough to be neglected and then the Seebeck coefficient depends only on the carriers concentration. We have calculated a fraction of occupied sites for $LaNi_{0.75}W_{0.25}O_3$ of 0.45. This value is clearly much greater than that expected from the only contribution of doping. This result has been previously interpreted for similar systems as indicative of a complex conduction mechanism, which includes intermediate behavior between a metal and a semiconductor (23).

In Fig. 10, we propose a band model for the title compounds, having in mind all the results mentioned above.

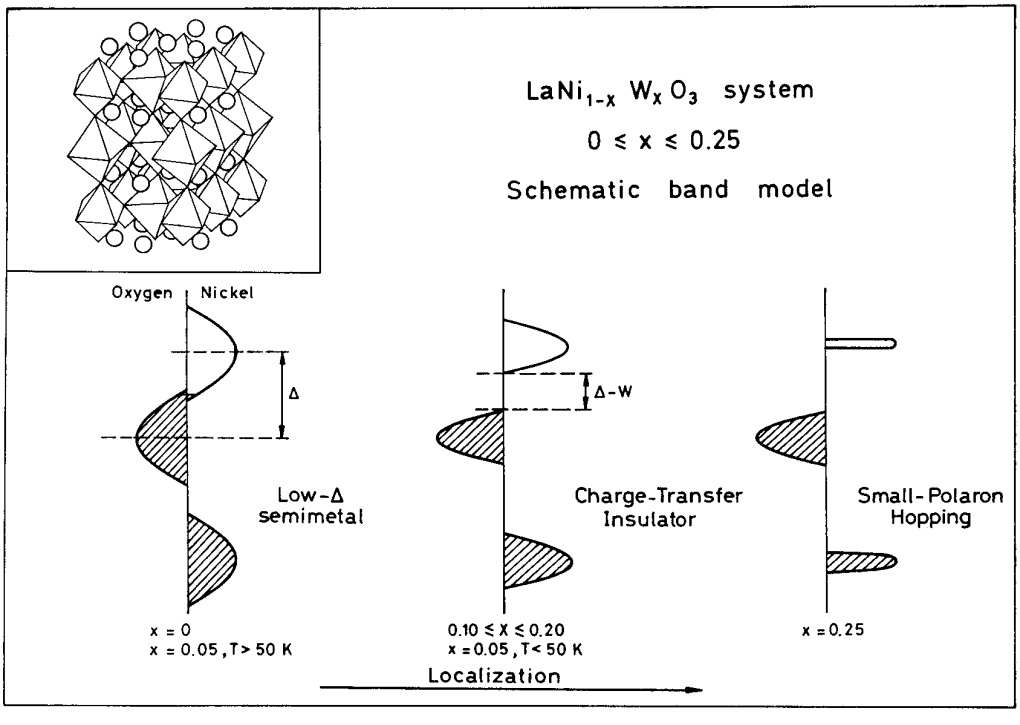

FIG. 10. Proposed schematic band model for $LaNi_{1-x}W_xO_3$. The inset shows the perovskite structure of the title compounds.

The electronic behavior of these materials as a function of composition and temperature can be qualitatively explained as follows:

In the sample with $x = 0$, metallic behavior is observed and its conductivity values correspond typically to correlated systems. The formal substitution of nickel cations by tungsten ones in the structure introduces changes in this respect. For the composition $x = 0.05$ the same behavior as that for $x = 0$ is preserved above ~50 K whereas at lower temperatures the bands seem to be not large enough to allow metallic conduction. This transition could be probably due to entropic effects as the temperature increases, allowing a better overlapping of orbitals, which give rise to a narrow conduction band. This fact is in good agreement with the observed dependence of θ_1 and θ_2 values on temperature for the oxide with $x = 0.20$. As temperature is increased, these angles are also increased and, in this sense, the overlapping between Ni/W atom *d* orbitals with the oxygen *p* orbitals is more effective, giving rise to larger bands which are responsible for the progressive tendency to metallic behavior as temperature is increased. Similar results have been previously reported for other systems, e.g., $RNiO_3$ perovskites (7). The obtained results could be taken into account as representative of the observed electrical behavior for the global title series as this progressive tendency to electronic delocalization with increasing temperature is observed in the whole series.

When x increases up to 0.20, the substitutional effects are more marked and intermediate behavior between metal and semiconductor is observed. Similar results have been previously found for systems near a M–I transition (5). As the doping level increases, a charge transference gap seems to appear as a consequence of the disorder introduced in the structure (tungsten-rich domains) and therefore greater localization of levels would take place. Similar results have been reported for related systems (7). Finally, when $x = 0.25$, the system rises to the limit of the insulating side of this transition, and the conduction process could occur via a hopping mechanism. This mechanism would suggest the presence of an important electronic localization as a consequence of the lattice polarization.

In conclusion, the electronic characterization of the $LaNi_{1-x}W_xO_3$ system shows the presence of temperature and composition M–I transitions. The temperature dependence of the observed electronic behavior has been explained in relation to the increase of θ_1 and θ_2 values with temperature. As pointed out before (4, 7, 24), these angles are, in a great manner, responsible for the more or less effectivity in the orbitals overlapping. In this sense, the observed variation suggests that, as temperature increases, larger bands are built and a progressive tendency to the metallic state takes place in the title system.

On the other hand, the composition dependence of the electronic behavior for these materials has been interpreted in terms of the progressive localization introduced as the substitution level, x, is increased.

ACKNOWLEDGMENTS

We thank Dr. M. T. Fernández (Institut Laue-Langevin, Grenoble, France) for the assistance in the neutron diffraction measurements and for her helpful comments. This work was supported by the CICYT (Projects PB92-0214 and MAT 92-0374) (Spain).

REFERENCES

1. Z. Zhang and M. Greenblatt, *J. Solid State Chem.* **111,** 141 (1994).
2. Z. Zhang, M. Greenblatt, and J. B. Goodenough, *J. Solid State Chem.* **108,** 402 (1994).
3. K. Sreedhar, M. McElfresh, D. Perry, D. Kim, P. Metcalf, and J. M. Honig, *J. Solid State Chem.* **110,** 208 (1994).
4. J. B. Torrance, P. Lacorre, A. I. Nazzal, E. J. Ansaldo, and Ch. Niedermayer, *Phys. Rev. B* **45** (14), 8209 (1992).
5. K. P. Rajeev and A. K. Raychaudhuri, *Phys. Rev. B* **46**(3), 1309 (1992).
6. C. N. R. Rao, O. M. Parkash, and P. Ganguly, *J. Solid State Chem.* **15,** 186 (1975).
7. J. B. Torrance, P. Lacorre, C. Asavaroengchai, and R. M. Metzger, *J. Solid State Chem.* **90,** 168 (1991), and references therein.
8. B. W. Arbuckle, K. V. Ramanujachary, Z. Zhang, and M. Greenblatt, *J. Solid State Chem.* **88,** 278 (1990).
9. K. Sreedhar and J. M. Honig, *J. Solid State Chem.* **111,** 147 (1994).
10. P. Dougier and P. Hagenmuller, *J. Solid State Chem.* **15,** 158 (1975).
11. H. Takagi, T. Ido, S. Ishibashi, M. Uota, and S. Uchida, *Phys. Rev. B* **40,** 2254 (1989).
12. K. P. Rajeev, G. V. Shivashankar, and A. K. Raychaudhuri, *Solid State Commun.* **79**(7), 591 (1991).
13. J. K. Vassiliou, M. Hornbostel, R. Ziebarth, and F. J. Disalvo, *J. Solid State Chem.* **81,** 208 (1989).
14. I. Alvarez, M. L. Veiga, and C. Pico, *J. Mater. Chem.* **5,** 1049 (1995).
15. J. Rodríguez-Carvajal, "Program Fullprof." Grenoble, France, 1994.
16. L. J. Van der Pauw, *Philips Res. Rep.* **1,** 13 (1958).
17. R. D. Shannon, *Acta Crystallogr. Sect. A* **32,** 751 (1976).
18. M. Medarde, A. Fontaine, J. L. García-Muñoz, J. Rodríguez-Carvajal, M. de Santis, M. Sacchi, G. Rossi, and P. Lacorre, *Phys. Rev. B* **46**(23), 14975 (1992).
19. A. K. Raychaudhuri, *Phys. Rev. B* **44**(16), 8572 (1991).
20. P. A. Cox, "Transition Metal Oxides. An Introduction to Their Electronic Structure and Properties." Clarendon Press, Oxford, 1992.
21. J. B. Goodenough, *Prog. Solid State Chem.* **5,** 238 (1971).
22. R. H. Heides and R. W. Ure, "Thermoelectricity." Interscience, New York, 1961.
23. J. H. Kuo, H. U. Anderson, and D. Sparlin, *J. Solid State Chem.* **87,** 55 (1990); F. R. Van Buren and J. H. W. De Wit, *J. Electrochem. Soc.* **126,** 1817 (1979).
24. J. Zaanen, G. A. Sawatzky, and J. W. Allen, *Phys. Rev. Lett.* **55,** 418 (1985).